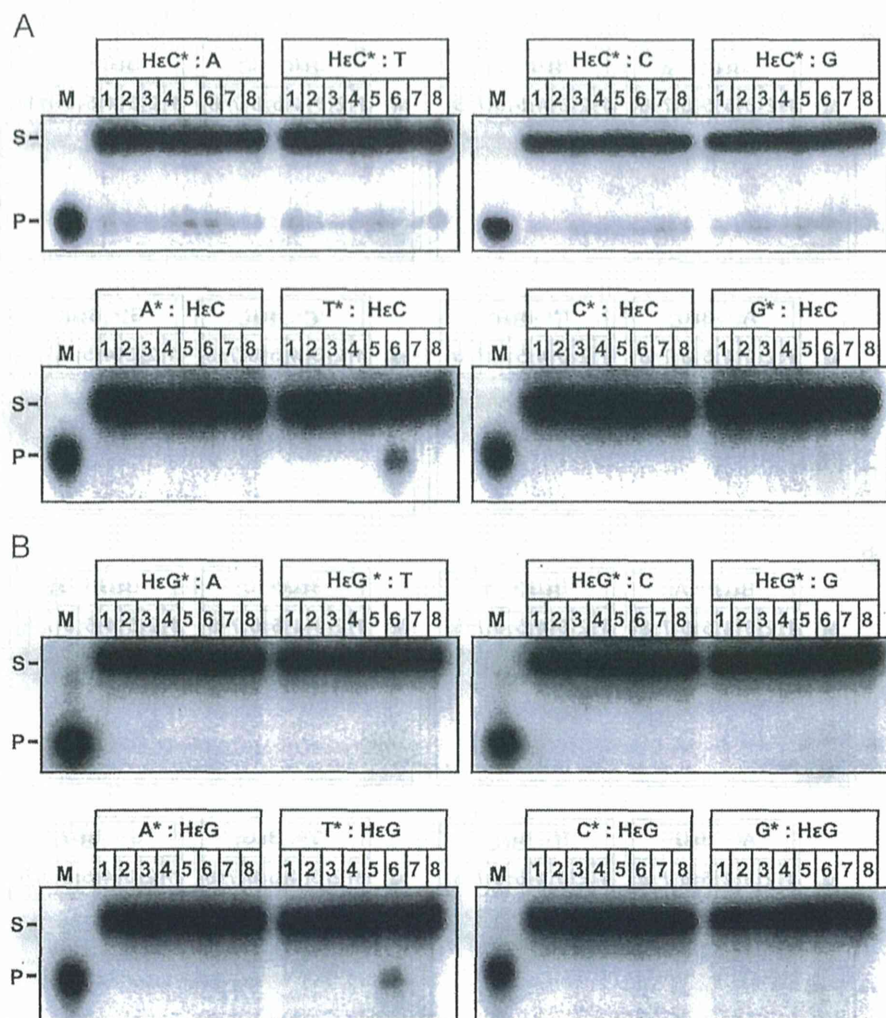

Fig. 3. Evaluation of repair activities of 8 DNA glycosylase proteins against 4-oxo-nonenal adducts. The abilities of the DNA glycosylase proteins OGG1, SMUG1, NTH1, UNG2, MPG, TDG, MUTYH, and NEIL1 to repair double-stranded DNA containing heptanone-ethenocytosine (HεC) (A) or heptanone-ethenoguanine (HεG) (B) were examined using a DNA cleavage assay. Each BER protein (300 fmol) was allowed to act on a double-stranded oligonucleotide containing HεC or HεG at 37 °C for 30 min. The asterisks show the 5′-labeled ^{32}P-labeled oligonucleotides, consisting of HεC-containing or HεG-containing oligonucleotides in the upper panels of (A) and (B), respectively, and unmodified oligonucleotides in the lower panels of (A) and (B). Numbers 1, 2, 3, 4, 5, 6, 7, and 8 indicate OGG1, SMUG1, NTH1, UNG2, MPG, TDG, MUTYH, and NEIL1, respectively. A ^{32}P-labeled marker oligonucleotide was used as a size marker for the cleavage products. The intact 30-mer oligonucleotides (substrate) and cleavage products are indicated by S and P, respectively.

cells ($20.5 \pm 15.2 \times 10^{-3}$) was 1.5-fold higher than that in the control cells ($14.0 \pm 6.8 \times 10^{-3}$), but the difference did not reach statistical significance. Next, the mutation spectra of the *supF* gene in plasmids treated at CAA in the control and the TDG-knockdown cells were examined using PCR and subsequencing analyses (Fig. 7B). First, the PCR-amplified products of the *supF* region were subjected to agarose gel electrophoresis; almost all the products showed the same mobility as a wild-type *supF* clone, indicating that most of the mutations were likely to be base substitutions or small insertions or deletions. Further sequencing analysis of the PCR products revealed that almost all the products showing the same mobility as a wild-type *supF* clone were actually base substitution-type mutations, but the mutation spectra differed between the control and the TDG-knockdown cells. Interestingly, modest increases of G:C to T:A transversion and G:C to A:T transition were found in TDG-knockdown cells (i.e., the proportions of G:C to T:A transversions in TDG-knockdown and control cells were 46.4% and 42.3%, respectively, and the proportions of G:C to A:T transitions in TDG-knockdown and control cells were 32.1% and 26.9%, respectively), but this difference was not statistically significant. Thus, the role of TDG in suppressing mutations caused by εC in human cells may be modest.

Discussion

εA, εC, N^2,3-ethenoguanine (N^2,3-εG), and 1,N^2-ethenoguanine (1,N^2-εG) in etheno-DNA adducts are reported to be repaired in *E. coli* and human BER pathways by several groups [40]. However, the repair systems of BεC, BεG, HεC, and HεG recently found in human tissues have not been investigated yet. In addition, although a BER enzyme MUTYH is known to catalyze the removal of adenine mispaired with 8-hydroxyguanine (8OHG), which is an oxidized form of guanine and is highly mutagenic, in double-stranded DNA and to prevent G:C to T:A mutations at 8OHG site, the repair functions of DNA glycosylase proteins against opposite bases of etheno-DNA adducts have not been fully examined. In this study, we newly found that in addition to its direct repair activity against εC, the human BER enzyme TDG is also capable of removing thymine mispaired with εC, BεC, BεG, HεC, and HεG *in vitro*. We also revealed that TDG in human cells is involved in the promotion of cell death caused by inducers of etheno-DNA adducts, the removal of εC, and the suppression of G:C to T:A and G:C to A:T mutation by comparing the TDG-knockdown cell line and its control cell line. These results suggested that TDG is involved in the repair of etheno-DNA adducts in human cells *in vivo*.

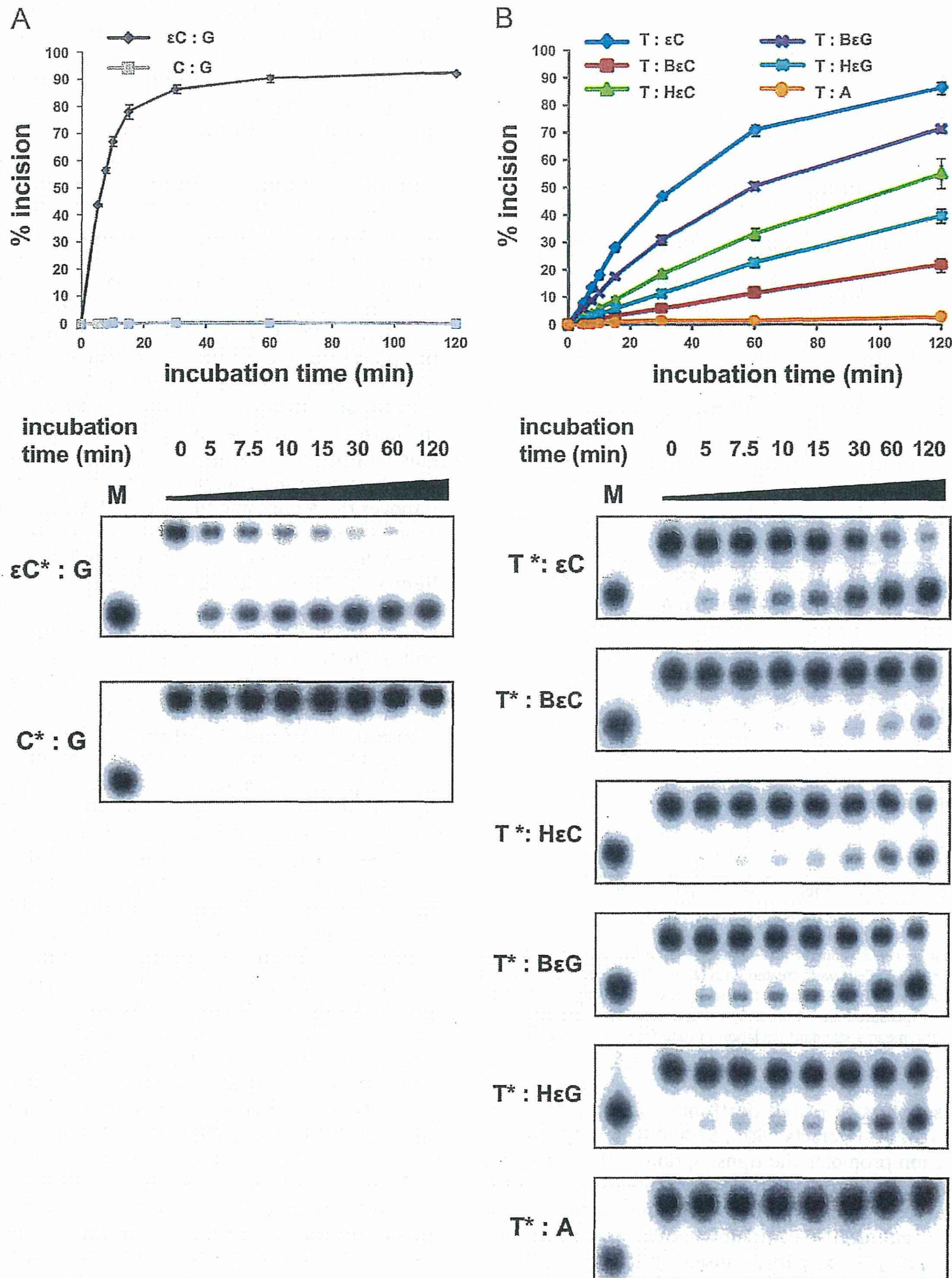

Fig. 4. Time-course assay for cleavage of DNA containing an etheno adduct by TDG protein. (A) Time-course assay for the cleavage of DNA containing εC:G and C:G base pairs by TDG protein. TDG protein (300 fmol) was incubated at 37 °C for 0–120 min with double-stranded oligonucleotides containing εC:G and C:G base pairs (50 fmol). The amount of cleavage products as a proportion of the total oligonucleotides was calculated as the % incision. The % incision valves are shown as the means ± standard deviations of data from three independent experiments. The lower panels show representative results of the DNA cleavage assays of TDG protein. (B) Time-course assay of the cleavage of DNA containing T:εC, T:BεC, T:BεG, T:HεC, T:HεG, and T:A base pairs by TDG protein. TDG protein (300 fmol) was incubated at 37 °C for 0–120 min with double-stranded oligonucleotides containing T:εC, T:BεC, T:BεG, T:HεC, T:HεG, and T:A (50 fmol). The lower panels show representative results of the DNA cleavage assays for TDG protein.

In our cell survival assay, the proportion of cells that survived was significantly lower in the control cells than in the TDG-knockdown cells when exposed to a higher dose of CAA, 4-ONE, and 4-OHE. This result raises the possibility that TDG may be involved in the induction of the plural cell death mechanism. Kunz et al. [41] previously reported that immortalized mouse embryonic fibroblasts (MEFs) derived from $Tdg^{-/-}$ mice and TDG-knockdown cells from a human cancer cell line exhibited an increase in resistance of 5-FU that is one of substrate on TDG. The loss of TDG induces XRCC1 foci, which enhances single-stranded DNA break repair activity, after 5-FU treatment and is thought to reduce lethal 5-FU processing. Our finding that TDG-knockdown cells are resistant to cell death after treatment with an inducer of etheno-DNA adducts is also suspected to be caused by a mechanism

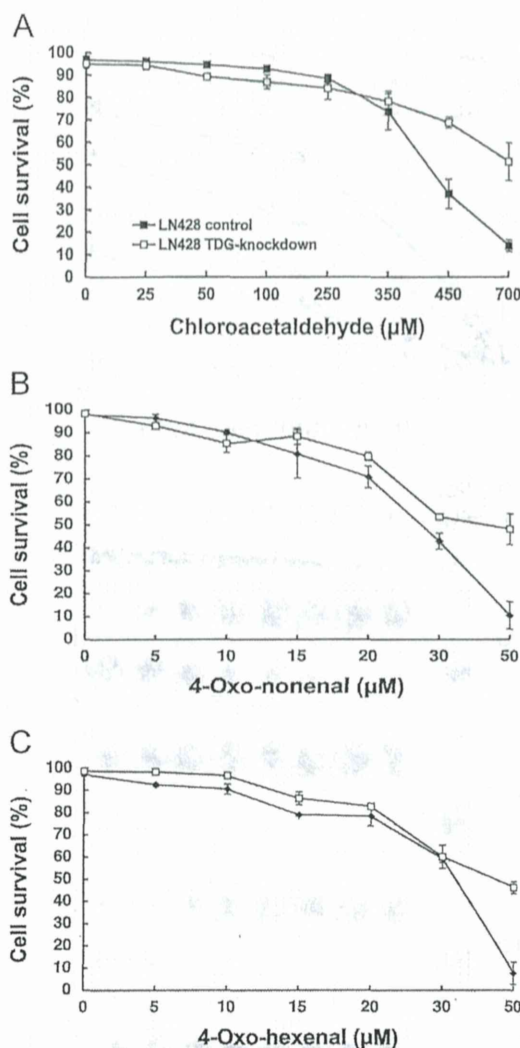

Fig. 5. Cell survival of LN428-control and LN428-TDG-knockdown cells treated with CAA, 4-ONE, or 4-OHE. Cells were treated with (A) 0–700 μM CAA, (B) 0–50 μM 4-ONE, or (C) 0–50 μM 4-OHE for 2 h; after the medium was exchanged with fresh medium, survival was measured after 12 h using a trypan blue exclusion assay. The % of cell survival is the mean ± standard deviation of data from 2 to 3 independent experiments.

similar to the suppression of cell death observed in 5-FU treatment. In addition, TDG interacts with p53 and its family proteins, and this interaction promotes the transcription of the p53 family downstream genes when p53 and its family proteins are activated [42]. Since the p53 family proteins regulate apoptosis, the decreased cell death in TDG-knockdown cells, compared with control cells, is likely to be partly caused by the fact that p53 family proteins cannot interact with the TDG protein. From the result that TDG-knockdown cells were more viable than control cells when exposed to an etheno-DNA adduct inducer, we assumed that those cells with a lower TDG expression, abundant etheno-DNA adducts, and subsequent abundant mutations may have greater chance to survive or to gain disease-causing mutations. Thus, the maintenance of the TDG expression level is likely to be important in human cells, especially during exposure to severe oxidative stresses. LN428 cells with or without TDG expression began to die when treated with comparatively low doses of 4-ONE or 4-OHE. We do not know the exact underlying mechanism, but it is known that the unmodified base mispaired with exocyclic base is recognized by mismatch repair (MMR) enzymes as well as by BER enzymes [43]. Since MMR proteins reportedly interact with translesion DNA synthesis (TLS) polymerase [44], this polymerase may also play a direct role in the repair process of etheno-DNA adducts. Exocyclic DNA adducts, such as HεC, can inhibit function of TLS DNA polymerase and strongly block DNA synthesis [45]. Thus, the repair of etheno-DNA adducts by the MMR system may also create a persistent single-strand break and induce cell death.

TDG was shown to have two kinds of functions against εC repair in this study: the excision of εC from εC:G base pairs in double-stranded DNA, and the removal of thymine mispaired with εC in double-stranded DNA. εC is highly mutagenic and causes C:G to A:T transversions or C:G to T:A transitions in *E. coli* and mammalian cells [46,47]; thus it may wrongly pair with thymine or adenine bases during DNA replication. In the case of εC:T mispairing, TDG is predicted to remove T, but the consequence of this process is different depending on which base is opposed to εC after T excision. For example, when DNA polymerase works and fills the gap with G, εC:T is changed to εC:G, and finally, restored to the normal C:G base pair by authentic function of TDG or SMUG1. This TDG activity of removal of the base opposing to the adducted base, here reported, reminds us of the behavior of MUTYH, which removes the A opposing to 8-OHG. This function implies that TDG plays an important role in preventing mutations against εC, especially C:G to A:T transversions. When the DNA polymerase inserts T, DNA containing εC falls into a futile repair cycle, and suffers from persistent single-strand break. If the polymerase inserts A and C, εC:T base pairs may cause C:G to T:A mutation and C:G to G:C mutation, respectively. An assay employing shuttle vector plasmid containing HεC has been reported that HεC blocked DNA synthesis and brought many mutations in human cells [45]. The miscoding frequency was higher than 90% and T and A were preferentially inserted to the place opposite to the adduct. Therefore, we assume that the mutations caused by HεC can also be prevented by TDG. The position where the bases were removed by TDG are reportedly reconstituted by BER pathway-related enzymes including DNA polymerase beta [48]. In future studies, we would like to clarify the details on how TDG and its related enzymes work after T against etheno-DNA adduct was removed.

In this paper, the *supF* forward mutation assay showed a modest increase in the proportion of G:C to T:A (C:G to A:T) mutations and G:C to A:T (C:G to T:A) mutations in CAA-treated TDG-knockdown cells than in control cells with the same treatment (Fig. 7B), and these mutation spectra are known to be caused by εC. The observation that the increase was not statistically significant in our experiment is thought to have been due to the effect of other DNA adducts generated by CAA, because it has been reported that CAA treatment generates not only εC DNA adducts, but also other DNA adducts, such as εG, in DNA [49].

In our quantitative analysis of adduct level in transfected plasmids (Fig. 6A), the εdC levels of plasmids transfected into TDG-knockdown cells were higher than those of plasmids transfected into control cells. The reduced repair activity of TDG toward εC in TDG-knockdown cells may compensate the ordinary power to reduce εdC levels in the cells. Molatore et al. [50] and Turco et al. [51] have reported that the 8OHG levels in immortalized MEFs derived from Mutyh-/- mice were higher than in wild-type MEFs after exposure to $KBrO_3$, a base damage inducer. The results of both papers suggest that a difference in DNA glycosylase activity toward unmodified bases paired with modified bases in cells can lead to the differences in the modified adduct levels in the cells. Like the findings in their reports, if TDG repairs the mispairing of εC:T to εC:G, the loss of this function of TDG itself may also contribute to the remaining εdC levels in TDG-knockdown cells.

In our DNA cleavage assay with control lane in which oligonucleotide was treated only with alkali (Supplementary Fig. S3), it was found that background signal due to alkali treatment was seen in the lanes of reaction of DNA glycosylase and substrate oligonucleotide. It is known

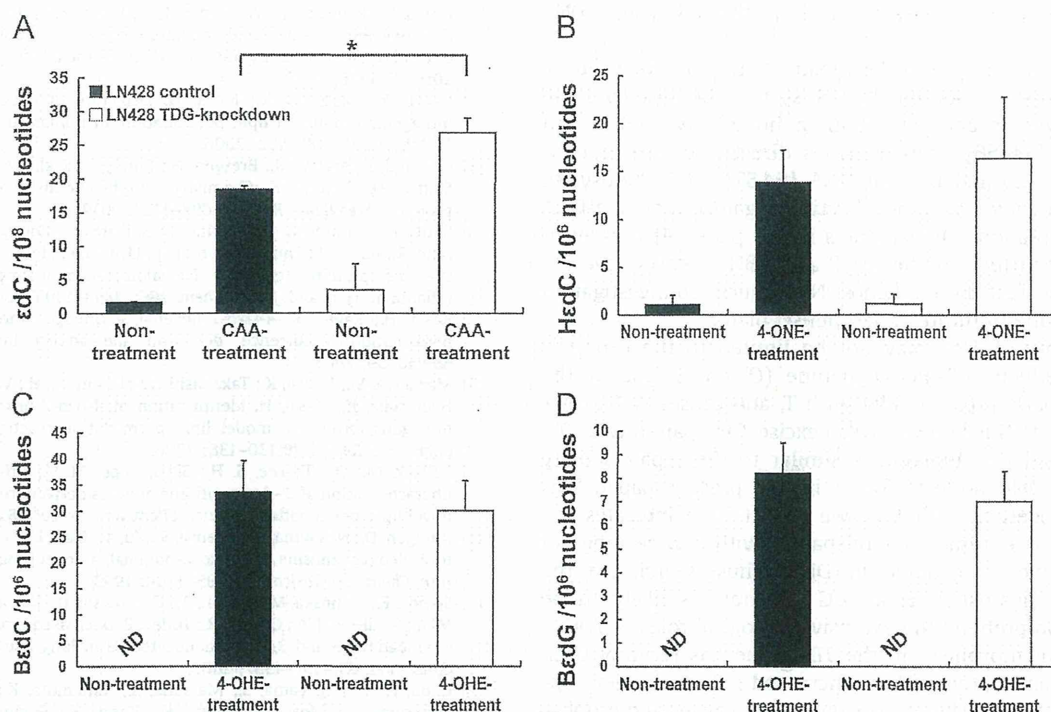

Fig. 6. Measurement of repair activity against etheno-DNA adducts in LN428-control and LN428-TDG-knockdown cells. Adduct-modified pEGFP plasmids were transfected into the cells; after incubation for 24 h, the plasmids were collected and the levels of εdC (A), HεdC (B), BεdC (C), and BεdG (D) were measured using LC-MS/MS. Values are the means ± standard deviations of three measurements. *P* values were calculated using a two-tailed Student *t* test, $^{*}P < 0.05$. ND means not detected.

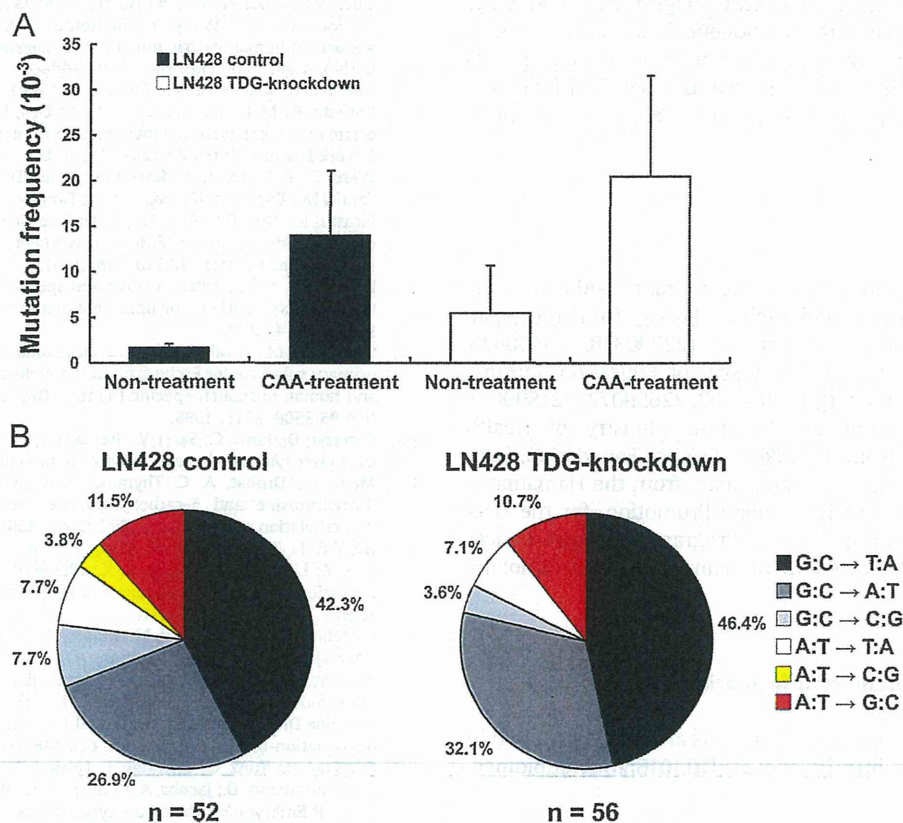

Fig. 7. *SupF* forward mutation assay using CAA-treated plasmid pMY189 in LN428-control and LN428-TDG knockdown cells. (A) The mutation frequency of the *supF* gene in pMY189 was measured using a *supF* forward mutation assay. The mutation frequency is shown as the mean ± standard deviation of data from 6 experiments. (B) Proportion of mutation spectrum of the *supF* gene in the CAA-treated pMY189 replicated in the control and TDG knockdown cells. The 'n' is the mutation number.

that etheno-DNA adducts are decomposed under alkaline conditions and converted into ring-opened structures [46,52,53]. Since the background bands are found in the lane of an oligonucleotide treated only with alkali, decomposition of etheno-DNA adducts can be presumed to generate an apurinic/apyrimidinic site. Interestingly, alkali treatment against etheno-DNA adducts seems to have a stronger influence on

the cytosine-DNA adducts, in particular on εC, than on guanine-DNA adducts.

There is nothing simple in the repair of etheno-DNA adducts. εA and εC are repaired not only by BER systems but also by *E. coli* AlkB family proteins and their human homologues ABH2 and ABH3 proteins [54–56]. AlkB enzymes directly reverse etheno-DNA adducts to normal base in DNA [54,57]. DNA glycosylase proteins did not show the removal activity against butanone-DNA adducts and heptanone-DNA adducts in our paper. At present, it has not been reported whether AlkB and ABH proteins have the repair activity against these etheno-DNA adducts, so investigation of this point is one of future experimental plans.

Repair activity of TDG may not be limited to the exocyclic etheno-DNA adducts. O^6-Methylguanine (O^6-meG), one of the alkyl adducts, pairs preferentially with T, and causes G:C to A:T transitions [58]. TDG is known to also excise T mispaired with O^6-meG [59,60], and this function is similar to the repair activity against etheno-DNA adducts found in the present paper. This phenomenon together with that we report here indicates the possibility that TDG removes T mispaired with a wide range of modified cytosine or guanine in DNA. Thus, search for the modified bases against T as a TDG substrate is likely to be important to comprehend the extensive biological roles of TDG.

A genetic polymorphism in the *TDG* gene has recently been reported to be associated with an increased risk of the development of nonmelanoma skin cancer plus other cancer and esophageal squamous cell carcinomas [61,62]. In addition, the loss of heterozygosity of the *TDG* gene, which is located at chromosome 12q24.1, has been detected in gastric cancers [63]. These genetic alterations of the *TDG* gene in cancer suggest that TDG plays important roles in preventing carcinogenesis in various human organs. The DNA repair activity of TDG, shown in previous papers [48,64] and in the current study, as well as other TDG functions, such as DNA demethylation, may be involved in such cancer-preventing roles.

Acknowledgments

This work was supported in part by a Grant-in-Aid from the Ministry of Health, Labour, and Welfare (21-1), from the Japan Society for the Promotion of Science [22790378, 25460476, 22659072, 24659161], from the Ministry of Education, Culture, Sports, Science, and Technology [20014007, 22659072, 221S0001], for Cancer Research from the Japanese Ministry of Health [23120201, 10103838], from the Takeda Science Foundation, from Center of Innovation Program of JST, Japan, from the Hamamatsu Foundation for Science and Technology Promotion, for the U.S.-Japan Cooperative Medical Science Program, National Cancer Center Research and Development Fund, and the Smoking Research Foundation.

Appendix A. Supplementary Information

Supplementary data associated with this article can be found in the online version at http://dx.doi.org/10.1016/j.freeradbiomed.2014.07.044.

References

[1] Nair, U.; Bartsch, H.; Nair, J. Lipid peroxidation-induced DNA damage in cancer-prone inflammatory diseases: a review of published adduct types and levels in humans. *Free Radic. Biol. Med.* **43**:1109–1120; 2007.
[2] Brash, A. R. Lipoxygenases: occurrence, functions, catalysis, and acquisition of substrate. *J. Biol. Chem.* **274**:23679–23682; 1999.
[3] Lee, S. H.; Rangiah, K.; Williams, M. V.; Wehr, A. Y.; DuBois, R. N.; Blair, I. A. Cyclooxygenase-2-mediated metabolism of arachidonic acid to 15-oxo-eicosatetraenoic acid by rat intestinal epithelial cells. *Chem. Res. Toxicol.* **20**:1665–1675; 2007.
[4] Kawai, K.; Matsuno, K.; Kasai, H. Detection of 4-oxo-2-hexenal, a novel mutagenic product of lipid peroxidation, in human diet and cooking vapor. *Mutat. Res.* **603**:186–192; 2006.
[5] Guéraud, F.; Atalay, M.; Bresgen, N.; Cipak, A.; Eckl, P. M.; Huc, L.; Jouanin, I.; Siems, W.; Uchida, K. Chemistry and biochemistry of lipid peroxidation products. *Free Radic. Res.* **44**:1098–1124; 2010.
[6] Shibata, T.; Shimozu, Y.; Wakita, C.; Shibata, N.; Kobayashi, M.; Machida, S.; Kato, R.; Itabe, H.; Zhu, X.; Sayre, LM.; Uchida, K. Lipid peroxidation modification of protein generates Nepsilon-(4-oxononanoyl)lysine as a pro-inflammatory ligand. *J. Biol. Chem.* **286**:19943–19957; 2011.
[7] Kasai, H.; Kawai, K. 4-Oxo-2-hexenal, a mutagen formed by omega-3 fat peroxidation: occurrence, detection and adduct formation. *Mutat. Res.* **659**:56–59; 2008.
[8] Maekawa, M.; Kawai, K.; Takahashi, Y.; Nakamura, H.; Watanabe, T.; Sawa, R.; Hachisuka, K.; Kasai, H. Identification of 4-oxo-2-hexenal and other direct mutagens formed in model lipid peroxidation reactions as dGuo adducts. *Chem. Res. Toxicol.* **19**:130–138; 2006.
[9] Pollack, M.; Oe, T.; Lee, S. H.; Silva, Elipe, M. V.; Arison, B. H.; Blair, I. A. Characterization of 2′-deoxycytidine adducts derived from 4-oxo-2-nonenal, a novel lipid peroxidation product. *Chem. Res. Toxicol.* **16**:893–900; 2003.
[10] Rindgen, D.; Nakajima, M.; Wehrli, S.; Xu, K.; Blair, I. A. Covalent modifications to 2′-deoxyguanosine by 4-oxo-2-nonenal, a novel product of lipid peroxidation. *Chem. Res. Toxicol.* **12**:1195–1204; 1999.
[11] Speina, E.; Zielińska, M.; Barbin, A.; Gackowski, D.; Kowalewski, J.; Graziewicz, M. A.; Siedlecki, J. A.; Oliński, R.; Tudek, B. Decreased repair activities of 1,N(6)-ethenoadenine and 3,N(4)-ethenocytosine in lung adenocarcinoma patients. *Cancer Res.* **63**:4351–4357; 2003.
[12] Chou, P. H.; Kageyama, S.; Matsuda, S.; Kanemoto, K.; Sasada, Y.; Oka, M.; Shinmura, K.; Mori, H.; Kawai, K.; Kasai, H.; Sugimura, H.; Matsuda, T. Detection of lipid peroxidation-induced DNA adducts caused by 4-oxo-2(E)-nonenal and 4-oxo-2(E)-hexenal in human autopsy tissues. *Chem. Res. Toxicol.* **23**:1442–1448; 2010.
[13] Matsuda, T.; Tao, H.; Goto, M.; Yamada, H.; Suzuki, M.; Wu, Y.; Xiao, N.; He, Q.; Guo, W.; Cai, Z.; Kurabe, N.; Ishino, K.; Matsushima, Y.; Shinmura, K.; Konno, H.; Maekawa, M.; Wang, Y.; Sugimura, H. Lipid peroxidation-induced DNA adducts in human gastric mucosa. *Carcinogenesis* **34**:121–127; 2013.
[14] Barbin, A. Formation of DNA etheno adducts in rodents and humans and their role in carcinogenesis. *Acta Biochim. Pol.* **45**:145–161; 1998.
[15] Boffetta, P.; Matisane, L.; Mundt, K. A.; Dell, L. D. Meta-analysis of studies of occupational exposure to vinyl chloride in relation to cancer mortality. *Scand. J. Work Environ. Health* **29**:220–229; 2003.
[16] Ward, E.; Boffetta, P.; Andersen, A.; Colin, D.; Comba, P.; Deddens, J. A.; De, Santis, M.; Engholm, G.; Hagmar, L.; Langard, S.; Lundberg, I.; McElvenny, D.; Pirastu, R.; Sali, D.; Simonato, L. Update of the follow-up of mortality and cancer incidence among European workers employed in the vinyl chloride industry. *Epidemiology* **12**:710–718; 2001.
[17] Bartsch, H.; Nair, J. Ultrasensitive and specific detection methods for exocylic DNA adducts: markers for lipid peroxidation and oxidative stress. *Toxicology* **153**:105–114; 2000.
[18] Saparbaev, M.; Laval, J. 3,N4-ethenocytosine, a highly mutagenic adduct, is a primary substrate for Escherichia coli double-stranded uracil-DNA glycosylase and human mismatch-specific thymine-DNA glycosylase. *Proc. Natl. Acad. Sci. USA* **95**:8508–8513; 1998.
[19] Cortázar, D.; Kunz, C.; Saito, Y.; Steinacher, R.; Schär, P. The enigmatic thymine DNA glycosylase. *DNA Repair (Amst.)* **6**:489–504; 2007.
[20] Maiti, A.; Drohat, A. C. Thymine DNA glycosylase can rapidly excise 5-formylcytosine and 5-carboxylcytosine: potential implications for active demethylation of CpG sites. *J. Biol. Chem.* **286**:35334–35338; 2011.
[21] He, Y. F.; Li, B. Z.; Li, Z.; Liu, P.; Wang, Y.; Tang, Q.; Ding, J.; Jia, Y.; Chen, Z.; Li, L.; Sun, Y.; Li, X.; Dai, Q.; Song, C. X.; Zhang, K.; He, C.; Xu, G. L. Tet-mediated formation of 5-carboxylcytosine and its excision by TDG in mammalian DNA. *Science* **333**:1303–1307; 2011.
[22] Cortellino, S.; Xu, J.; Sannai, M.; Moore, R.; Caretti, E.; Cigliano, A.; Le, Coz., M.; Devarajan, K.; Wessels, A.; Soprano, D.; Abramowitz, L. K.; Bartolomei, M. S.; Rambow, F.; Bassi, M. R.; Bruno, T.; Fanciulli, M.; Renner, C.; Klein-Szanto, A. J.; Matsumoto, Y.; Kobi, D.; Davidson, I.; Alberti, C.; Larue, L.; Bellacosa, A. Thymine DNA glycosylase is essential for active DNA demethylation by linked deamination-base excision repair. *Cell* **146**:67–79; 2011.
[23] Cortázar, D.; Kunz, C.; Selfridge, J.; Lettieri, T.; Saito, Y.; MacDougall, E.; Wirz, A.; Schuermann, D.; Jacobs, A. L.; Siegrist, F.; Steinacher, R.; Jiricny, J.; Bird, A.; Schär, P. Embryonic lethal phenotype reveals a function of TDG in maintaining epigenetic stability. *Nature* **470**:419–423; 2011.
[24] Wolfe, A. E.; O'Brien, P. J. Kinetic mechanism for the flipping and excision of 1, N(6)-ethenoadenine by human alkyladenine DNA glycosylase. *Biochemistry* **48**:11357–11369; 2009.
[25] Kavli, B.; Sundheim, O.; Akbari, M.; Otterlei, M.; Nilsen, H.; Skorpen, F.; Aas, P. A.; Hagen, L.; Krokan, H. E.; Slupphaug, G. hUNG2 is the major repair enzyme for removal of uracil from U:A matches, U:G mismatches, and U in single-stranded DNA, with hSMUG1 as a broad specificity backup. *J. Biol. Chem.* **277**:39926–39936; 2002.

[26] Rentel, C.; Wang, X.; Batt, M.; Kurata, C.; Oliver, J.; Gaus, H.; Krotz, A. H.; McArdle, J. V.; Capaldi, D. C. Formation of modified cytosine residues in the presence of depurinated DNA. *J. Org. Chem.* **70**:7841–7845; 2005.

[27] Raboisson, P.; Baurand, A.; Cazenave, J. P.; Gachet, C.; Retat, M.; Spiess, B.; Bourguignon, J. J. Novel antagonists acting at the P2Y(1) purinergic receptor: synthesis and conformational analysis using potentiometric and nuclear magnetic resonance titration techniques. *J. Med. Chem.* **45**:962–972; 2002.

[28] Shinmura, K.; Kasai, H.; Sasaki, A.; Sugimura, H.; Yokota, J. 8-Hydroxyguanine (7,8-dihydro-8-oxoguanine) DNA glycosylase and AP lyase activities of hOGG1 protein and their substrate specificity. *Mutat. Res.* **385**:75–82; 1997.

[29] Shinmura, K.; Tao, H.; Goto, M.; Igarashi, H.; Taniguchi, T.; Maekawa, M.; Takezaki, T.; Sugimura, H. Inactivating mutations of the human base excision repair gene NEIL1 in gastric cancer. *Carcinogenesis* **25**:2311–2317; 2004.

[30] Goto, M.; Shinmura, K.; Nakabeppu, Y.; Tao, H; Yamada, H.; Tsuneyoshi, T.; Sugimura, H. Adenine DNA glycosylase activity of 14 human MutY homolog (MUTYH) variant proteins found in patients with colorectal polyposis and cancer. *Hum. Mutat.* **31**:E1861–1874; 2010.

[31] Goto, M.; Shinmura, K.; Igarashi, H.; Kobayashi, M.; Konno, H.; Yamada, H.; Iwaizumi, M.; Kageyama, S.; Tsuneyoshi, T.; Tsugane, S.; Sugimura, H. Altered expression of the human base excision repair gene NTH1 in gastric cancer. *Carcinogenesis* **30**:1345–1352; 2009.

[32] Shinmura, K.; Goto, M.; Suzuki, M.; Tao, H.; Yamada, H.; Igarashi, H.; Matsuura, S.; Maeda, M.; Konno, H.; Matsuda, T.; Sugimura, H. Reduced expression of MUTYH with suppressive activity against mutations caused by 8-hydroxyguanine is a novel predictor of a poor prognosis in human gastric cancer. *J. Pathol.* **225**:414–423; 2011.

[33] Maciejewska, A. M.; Ruszel, K. P.; Nieminuszczy, J.; Lewicka, J.; Sokołowska, B.; Grzesiuk, E.; Kuśmierek, J. T. Chloroacetaldehyde-induced mutagenesis in Escherichia coli: the role of AlkB protein in repair of 3,*N*(4)-ethenocytosine and 3,*N*(4)-alpha-hydroxyethanocytosine. *Mutat. Res.* **684**:24–34; 2010.

[34] Roberts, D. W.; Churchwell, M. I.; Beland, F. A.; Fang, J. L.; Doerge, D. R. Quantitative analysis of etheno-2′-deoxycytidine DNA adducts using on-line immunoaffinity chromatography coupled with LC/ES-MS/MS detection. *Anal. Chem.* **73**:303–309; 2001.

[35] Kato, T.; Totsuka, Y.; Ishino, K.; Matsumoto, Y.; Tada, Y.; Nakae, D.; Goto, S.; Masuda, S.; Ogo, S.; Kawanishi, M.; Yagi, T.; Matsuda, T.; Watanabe, M.; Wakabayashi, K. Genotoxicity of multi-walled carbon nanotubes in both in vitro and in vivo assay systems. *Nanotoxicology* **7**:452–461; 2013.

[36] Yamane, A.; Shinmura, K.; Sunaga, N.; Saitoh, T.; Yamaguchi, S.; Shinmura, Y.; Yoshimura, K.; Murakami, H.; Nojima, Y.; Kohno, T.; Yokota, J. Suppressive activities of OGG1 and MYH proteins against G:C to T:A mutations caused by 8-hydroxyguanine but not by benzo[a]pyrene diol epoxide in human cells in vivo. *Carcinogenesis* **24**:1031–1037; 2003.

[37] Saparbaev, M.; Kleibl, K.; Laval, J. Escherichia coli, Saccharomyces cerevisiae, rat and human 3-methyladenine DNA glycosylases repair 1,*N*6-ethenoadenine when present in DNA. *Nucleic Acids Res.* **23**:3750–3755; 1995.

[38] An, Q.; Robins, P.; Lindahl, T.; Barnes, D. E. 5-Fluorouracil incorporated into DNA is excised by the Smug1 DNA glycosylase to reduce drug cytotoxicity. *Cancer Res.* **67**:940–945; 2007.

[39] Foiles, P. G.; Miglietta, L. M.; Nishikawa, A.; Kuśmierek, J. T.; Singer, B.; Chung, F. L. Development of monoclonal antibodies specific for 1,*N*2-ethenodeoxyguanosine and *N*2,3-ethenodeoxyguanosine and their use for quantitation of adducts in G12 cells exposed to chloroacetaldehyde. *Carcinogenesis* **14**:113–116; 1993.

[40] Gros, L.; Ishchenko, A. A.; Saparbaev, M. Enzymology of repair of etheno-adducts. *Mutat. Res.* **29**:219–229; 2003.

[41] Kunz, C.; Focke, F.; Saito, Y.; Schuermann, D.; Lettieri, T.; Selfridge, J.; Schär, P. Base excision by thymine DNA glycosylase mediates DNA-directed cytotoxicity of 5-fluorouracil. *PLoS Biol.* **7**:e91; 2009.

[42] Kim, E. J.; Um, S. J. Thymine-DNA glycosylase interacts with and functions as a coactivator of p53 family proteins. *Biochem. Biophys. Res. Commun.* **377**:838–842; 2008.

[43] Johnson, K. A.; Mierzwa, M. L.; Fink, S. P.; Marnett, L. J. MutS recognition of exocyclic DNA adducts that are endogenous products of lipid oxidation. *J. Biol. Chem.* **274**:27112–27118; 1999.

[44] Lv, L.; Wang, F.; Ma, X.; Yang, Y.; Wang, Z.; Liu, H.; Li, X.; Liu, Z.; Zhang, T.; Huang, M.; Friedberg, E. C.; Tang, T. S.; Guo, C. Mismatch repair protein MSH2 regulates translesion DNA synthesis following exposure of cells to UV radiation. *Nucleic Acids Res.* **41**:10312–10322; 2013.

[45] Pollack, M.; Yang, I. Y.; Kim, H. Y.; Blair, I. A.; Moriya, M. Translesion DNA Synthesis across the heptanone-etheno-2′-deoxycytidine adduct in cells. *Chem. Res. Toxicol.* **19**:1074–1079; 2006.

[46] Basu, A. K.; Wood, M. L.; Niedernhofer, L. J.; Ramos, L. A.; Essigmann, J. M. Mutagenic and genotoxic effects of three vinyl chloride-induced DNA lesions: 1,*N*6-ethenoadenine, 3,*N*4-ethenocytosine, and 4-amino-5-(imidazol-2-yl) imidazole. *Biochemistry* **32**:12793–12801; 1993.

[47] Moriya, M.; Zhang, W.; Johnson, F.; Grollman, A. P. Mutagenic potency of exocyclic DNA adducts: marked differences between Escherichia coli and simian kidney cells. *Proc. Natl. Acad. Sci. USA* **91**:11899–11903; 1994.

[48] Talhaoui, I.; Couvé, S.; Ishchenko, A. A.; Kunz, C.; Schär, P.; Saparbaev, M. 7,8-Dihydro-8-oxoadenine, a highly mutagenic adduct, is repaired by Escherichia coli and human mismatch-specific uracil/thymine-DNA glycosylases. *Nucleic Acids Res.* **41**:912–923; 2013.

[49] Kim, M. Y.; Zhou, X.; Delaney, J. C.; Taghizadeh, K.; Dedon, P. C.; Essigmann, J. M.; Wogan, G. N. AlkB influences the chloroacetaldehyde-induced mutation spectra and toxicity in the pSP189 supF shuttle vector. *Chem. Res. Toxicol.* **20**:1075–1083; 2007.

[50] Molatore, S.; Russo, M. T.; D'Agostino, V. G.; Barone, F.; Matsumoto, Y.; Albertini, A. M.; Minoprio, A.; Degan, P.; Mazzei, F.; Bignami, M.; Ranzani, G. N. MUTYH mutations associated with familial adenomatous polyposis: functional characterization by a mammalian cell-based assay. *Hum. Mutat.* **31**:159–166; 2010.

[51] Turco, E.; Ventura, I.; Minoprio, A.; Russo, M. T.; Torreri, P.; Degan, P.; Molatore, S.; Ranzani, G. N; Bignami, M; Mazzei, F. Understanding the role of the Q338H MUTYH variant in oxidative damage repair. *Nucleic Acids Res.* **41**:4093–4103; 2013.

[52] Basu, A. K.; Niedernhofer, L. J.; Essigmann, J. M. Deoxyhexanucleotide containing a vinyl chloride induced DNA lesion, 1,*N*6-ethenoadenine: synthesis, physical characterization, and incorporation into a duplex bacteriophage M13 genome as part of an amber codon. *Biochemistry* **26**:5626–5635; 1987.

[53] Speina, E.; Ciesla, J. M.; Wojcik, J.; Bajek, M.; Kusmierek, J. T.; Tudek, B. The pyrimidine ring-opened derivative of 1,*N*6-ethenoadenine is excised from DNA by the Escherichia coli Fpg and Nth proteins. *J. Biol. Chem.* **276**:21821--21827; 2001.

[54] Delaney, J. C.; Smeester, L.; Wong, C.; Frick, L. E.; Taghizadeh, K.; Wishnok, J. S.; Drennan, C. L.; Samson, L. D.; Essigmann, J. M. AlkB reverses etheno DNA lesions caused by lipid oxidation in vitro and in vivo. *Nat. Struct. Mol. Biol.* **12**:855–860; 2005.

[55] Ringvoll, J.; Moen, M. N.; Nordstrand, L. M.; Meira, L. B.; Pang, B.; Bekkelund, A.; Dedon, P. C.; Bjelland, S.; Samson, L. D.; Falnes, P.Ø.; Klungland, A. AlkB homologue 2-mediated repair of ethenoadenine lesions in mammalian DNA. *Cancer Res.* **68**:4142–4149; 2008.

[56] Fu, D.; Samson, L. D. Direct repair of 3,*N*(4)-ethenocytosine by the human ALKBH2 dioxygenase is blocked by the AAG/MPG glycosylase. *DNA Repair (Amst.)* **11**:46–52; 2012.

[57] Mishina, Y.; Yang, C. G.; He, C. Direct repair of the exocyclic DNA adduct 1,*N*6-ethenoadenine by the DNA repair AlkB proteins. *J. Am. Chem. Soc.* **127**:14594--14595; 2005.

[58] Fahrer, J.; Kaina, B. O6-methylguanine-DNA methyltransferase in the defense against N-nitroso compounds and colorectal cancer. *Carcinogenesis* **34**:2435--2442; 2013.

[59] Lari, S. U.; Day, R. S.; Dobler, K.; Paterson, M. C. Initiation of strand incision at G:T and *O*(6)-methylguanine:T base mismatches in DNA by human cell extracts. *Nucleic Acids Res.* **29**:2409–2417; 2001.

[60] Lari, S. U.; Al-Khodairy, F.; Paterson, M. C. Substrate specificity and sequence preference of G:T mismatch repair: incision at G:T, O6-methylguanine:T, and G:U mispairs in DNA by human cell extracts. *Biochemistry* **41**:9248–9255; 2002.

[61] Ruczinski, I.; Jorgensen, T. J.; Shugart, Y. Y.; Schaad, Y. B.; Kessing, B.; Hoffman-Bolton, J.; Helzlsouer, K. J.; Kao, W. H.; Wheless, L.; Francis, L.; Alani, R. M.; Strickland, P. T.; Smith, M. W.; Alberg, A. J. A population-based study of DNA repair gene variants in relation to non-melanoma skin cancer as a marker of a cancer-prone phenotype. *Carcinogenesis* **33**:1692–1698; 2012.

[62] Li, W. Q.; Hu, N.; Hyland, P. L.; Gao, Y.; Wang, Z. M.; Yu, K.; Su, H.; Wang, C. Y.; Wang, L. M.; Chanock, S. J.; Burdett, L.; Ding, T.; Qiao, Y. L.; Fan, J. H.; Wang, Y.; Xu, Y.; Shi, J. X.; Gu, F.; Wheeler, W.; Xiong, X. Q.; Giffen, C.; Tucker, M. A.; Dawsey, S. M.; Freedman, N. D.; Abnet, C. C.; Goldstein, A. M.; Taylor, P. R. Genetic variants in DNA repair pathway genes and risk of esophageal squamous cell carcinoma and gastric adenocarcinoma in a Chinese population. *Carcinogenesis* **34**:1536–1542; 2013.

[63] Schmutte, C.; Baffa, R.; Veronese, L. M.; Murakumo, Y.; Fishel, R. Human thymine-DNA glycosylase maps at chromosome 12q22-q24.1: a region of high loss of heterozygosity in gastric cancer. *Cancer Res.* **57**:3010–3015; 1997.

[64] Krokan, H. E.; Drabløs, F.; Slupphaug, G. Uracil in DNA—occurrence, consequences and repair. *Oncogene* **21**:8935–8948; 2002.

Gastric Cancer
DOI 10.1007/s10120-014-0409-4

ORIGINAL ARTICLE

Robust quantitative assessments of cytosine modifications and changes in the expressions of related enzymes in gastric cancer

Chunping Du · Nobuya Kurabe · Yoshitaka Matsushima · Masako Suzuki · Tomoaki Kahyo · Ippei Ohnishi · Fumihiko Tanioka · Shogo Tajima · Masanori Goto · Hidetaka Yamada · Hong Tao · Kazuya Shinmura · Hiroyuki Konno · Haruhiko Sugimura

Received: 17 April 2014 / Accepted: 13 July 2014
© The International Gastric Cancer Association and The Japanese Gastric Cancer Association 2014

Abstract
Background The rediscovery of 5-hydroxymethylcytosine, the ten-eleven translocation (*TET*) family, thymine-DNA glycosylase (*TDG*) and isocitrate dehydrogenase (*IDH*) have opened new avenues in the study of DNA demethylation pathways in gastric cancer (GC). We performed a comprehensive and robust analysis of these genes and modified cytosines in gastric cancer.
Methods Liquid chromatography mass spectrometry/mass spectrometry (LC-MS/MS) was used to assess 5-methyldeoxycytidine (5-mC), 5-hydroxymethyldeoxycytidine (5-hmC), 5-formyldeoxycytidine (5-fC) and 5-carboxyldeoxycytidine (5-caC) quantitatively in tumorous and non-tumorous regions of GCs; [D_2]-5-hmC was used as an internal standard. Expression levels of the genes *TET1*, *TET2*, *TET3*, *TDG*, *IDH1* and *IDH2* were measured using a real-time reverse transcription polymerase chain reaction (RT-PCR) and were compared to the clinical attributes of each case. Using HEK293T cells the effects of introducing plasmids containing full-length *TET1, TET2*, and *TET3* and 7 variants of the *TET2* catalytic domain were evaluated in terms of their effect on cytosine demethylation.
Results LC-MS/MS showed that 5-hmC was significantly decreased in tumorous portions. 5-mC was also moderately decreased in tumors, while 5-fC and 5-caC were barely detectable. The expressions of *TET1*, *TET2*, *TET3*, *TDG* and *IDH2*, but not *IDH1*, were notably decreased in GCs, compared with the adjacent non-tumor portion. *TET1*

C. Du and N. Kurabe contributed equally to this work.

Supplementary electronic material The online version of this article (doi:10.1007/s10120-014-0409-4) contains supplementary material available to authorized users.

C. Du · N. Kurabe · T. Kahyo · I. Ohnishi · S. Tajima · M. Goto · H. Yamada · H. Tao · K. Shinmura · H. Sugimura (✉)
Department of Tumor Pathology, Hamamatsu University School of Medicine, 1-20-1 Handayama, Higashi Ward, Hamamatsu, Shizuoka 431-3192, Japan
e-mail: hsugimur@hama-med.ac.jp

Y. Matsushima
Department of Chemistry, Hamamatsu University School of Medicine, Shizuoka, Japan

Present Address:
Y. Matsushima
Department of Applied Biology and Chemistry, Faculty of Applied Bioscience, Tokyo University of Agriculture, 1-1-1 Sakuragaoka, Setagaya-ku, Tokyo 156-8502, Japan

M. Suzuki
Research Equipment Center, Hamamatsu University School of Medicine, Shizuoka, Japan

I. Ohnishi · F. Tanioka
Iwata City Hospital, Iwata, Shizuoka, Japan

S. Tajima
Shizuoka Saiseikai Hospital, Shizuoka, Japan

Present Address:
M. Goto
Division of Cancer Development System, National Cancer Center Research Institute, 5-1-1 Tsukiji, Chuo-ku, Tokyo 104-0045, Japan

H. Konno
Department of Surgery II, Hamamatsu University School of Medicine, Shizuoka, Japan

Published online: 07 August 2014

expression and the 5-hmC levels determined using LC-MS/MS had a significantly positive correlation and TET1 protein had a greater effect on the increase in 5-hmC than TET2 and TET3 in HEK293T cells.

Conclusions The loss of 5-hmC and the down-regulation of *TET1-3*, *TDG* and *IDH2* were found in GCs. The loss of 5-hmC in GCs was mainly correlated with the down-regulation of *TET1*.

Keywords Cytosine modification · Liquid chromatography-mass spectrometry · $[D_2]$-5-hmC · Ten-eleven translocation family genes · Adductomics

Introduction

The ten-eleven translocation (TET) family proteins (TET1, TET2 and TET3) are responsible for the oxidation of 5-methylcytosine (5-mC) in DNA to 5-hydroxymethylcytosine (5-hmC) and the further oxidation of 5-hmC to 5-formylcytosine (5-fC) and 5-carboxylcytosine (5-caC), which are then cleaved from the DNA using thymine-DNA glycosylase (TDG) to be replaced with unmethylated cytosine [1–4]. Additionally, the oxidation reaction of TET proteins is dependent on Fe^{2+} and 2-oxoglutarate (2-OG), and 2-OG is dependent on the activity of isocitrate dehydrogenase IDH1 and IDH2 [5, 6] (Figure S1). The loss of 5-hydroxymethylcytosine and the down-regulation of the *TET* family and *IDH2* have been found in human cancers [7–11], but comprehensive evaluations of the modified cytosines and the enzymes that are involved have remained largely unperformed and most previous studies have used dot blot analyses as a means of measuring 5-hydroxymethyldeoxycytidine (5-hmC), which is at best a semi-quantitative method. Because dot blot analysis is based on the antigen-antibody reaction direct assessments of the absolute amount of 5-mC, 5-hmC, 5-fC, and 5-caC are not possible. Moreover, since the signal intensities of dot blot images become easily saturate, the standard curve used in the analyses is not linear [12]. In contrast to dot blot analysis, liquid chromatography coupled with tandem mass spectrometry (LC-MS/MS) can calculate the absolute quantity of the modifications and its standard curve is completely linear. Therefore, LC-MS/MS has greater sensitivity than dot blot analysis. Hence, we established an assay system using LC-MS/MS using a stable isotope standard to measure 4 modified deoxycytidines at the same time and these values were compared to the expression profiles of *TET1-3*, *TDG* and *IDH1-2*.

In this study we applied LC-MS/MS to assess 5-caC, 5-fC, 5-hmC and 5-mC in the genomic DNA of tumor portions and the corresponding non-tumor portions of gastric cancer (GC) samples. *TET1-3*, *TDG* and *IDH1-2* were quantitated using a real-time reverse transcription-polymerase chain reaction (RT-PCR). Next the coding exons of *TET*1-3 were analyzed by sequencing to search for possible somatic (tumor-specific) mutations and polymorphisms with neural or unknown functionality. Then we analyzed the effect of 5-mC oxidation *in vitro* by the introduction of *TET1-3* and 7 *TET2* variants into immortalized human embryonic kidney cells (HEK293T).

Materials and methods

Tissue samples and patients

GC tissues and the corresponding adjacent non-tumorous tissues from a total of 58 sporadic GC cases were obtained from the Hamamatsu University Hospital in Japan. The mean patient age was 66.9 years (SD 11.9 years) and the patients included 35 men and 23 women with 26 intestinal and 32 diffuse histological types. All cases were clinically operable and the stages ranged from I to III (no stage IV cases were included). Resected tissues, which were verified as tumorous regions (>70 %) or non-tumorous regions (no contamination with tumor cells) under a microscope by attending pathologists, were snap-frozen in liquid nitrogen and stored at −80 °C until used for the isolation of DNA and RNA. Histological classifications were based on the Japanese Classification of Gastric Carcinoma [13] and Lauren's classification [14] was applied when the cases were categorized into two types.

For comparison 5 pairs of gastric cancers and matched normal tissues from "Gan mice" (K19-Wnt1/C2mE), a kind gift of Prof. Masanobu Oshima at the Kanazawa University, were also used to measure these cytosine modifications in a non-human model of gastric cancer [15]. The project was approved by the Institutional Review Board of the Hamamatsu University School of Medicine (23-91).

Synthesis of stable isotope-labeled hmC and standard chemicals

Stable isotope-labeled 5-hydroxymethyl-2′-deoxycytidine ($[D_2]$-5-hmC) was synthesized from commercially available 5-iodo-2′-deoxycytidine (TCI, Tokyo Chemical Industry Co., Ltd., Tokyo, Japan) according to the literature [16]. 5-caC was also synthesized from commercially available 5-iodo-2′-deoxycytidine according to a previously reported protocol [17, 18]. 5-fC and 5-hmC were also synthesized from commercially available 5-mC (TCI) according to a previously reported protocol [19].

DNA purification and hydrolysis for LC-MS/MS

Genomic DNA was isolated and purified from samples of human gastric cancer. Approximately 100 mg of samples were homogenized with 600 μl of lysis solution (10 mM Tris-HCl [pH 8.0], 5 mM EDTA, 0.5 % SDS, and 0.01 % deferoxamine mesylate) using a Physcotron Handy Homogenizer NS-310EII (Microtech nichion, Chiba, Japan) at 15,000 rpm for 2 min. The homogenates were treated with 15 μl of protease K (QIAGEN, CA, USA) at 55°C for 3 h and 15 μl of RNase A (QIAGEN) at 37°C for 40 min. Two hundred microliters of protein precipitation solution (1 mM EDTA, 8 M ammonium acetate, 0.01 % deferoxamine mesylate) was added to the mixture followed by centrifugation at 14,000 g in room temperature for 5 min to remove proteins. Six hundred microliters of isopropanol was added to the supernatant and then centrifuged at 14,000 g in room temperature for 5 min to precipitate the genomic DNA. Precipitates were washed with 70 % ethanol and dried using a Speed-Vac concentrator (Savant, NY, USA). The dried genomic DNA was hydrated with distilled water at the concentration of about 1 mg/ml. Five micrograms of genomic DNA were treated with 50 U of DNaseI (New England Biosystems, MA, USA) for 30 min at 37 °C. After incubation 5 μg of phosphodiesterase I, 10 U of calf intestinal alkaline phosphatase (TaKaRa, Kyoto, Japan) and 10 ng of [D_2]-5-hmC were added to the mixture. After 1 h of incubation at 37 °C the proteins were removed using Nanosep 3K Omega (Pall Corp., MI, USA) by centrifugation at 14,000 g in 4 °C for 20 min. Digested samples were stored at −30 °C until used for LC-MS/MS analysis.

Quantification using LC-MS/MS

LC-MS/MS analyses were performed using a 4000 QTRAP mass spectrometer with an Acquity™ Ultra Performance LC system (AB SCIEX Instruments, Foster City, CA, USA). Digested DNA was injected and separated using an Acquity UPLC HSS T3 column (2.1 mm ×100 mm; Waters, Milford, CT, USA). The column was eluted as follows: deoxycytidine (C) and 5-mC were eluted in 94 % B from 0 to 3 min and in a linear gradient of 6–60 % B from 3 to 8 min at 0.2 mL/min; 5-hmC was eluted in 6 % B from 0 to 3 min and 20 % B from 3 to 8 min at 0.2 mL/min (mobile phase A: 0.02 % (v/v) acetic acid in water; mobile phase B: methanol); and 5-fC and 5-caC were eluted in 94 % B from 0 to 3 min and in a linear gradient of 6-20 % B from 3 to 10 min at 0.2 mL/min. Multi-reaction monitoring was performed in positive ion mode using nitrogen as the nebulizing gas. Experimental conditions were as follows: ion source temperature, 400°C; cone voltage, 5500 V; collision gas, nitrogen. Collision energies and characteristic reactions were as follows (collision energy (eV), base isonS→product ion): [D_2]-5-hmC (13 eV, 260.076→144.000), C (13 eV, 228.045→111.900), 5-mC (15 eV, 242.114→126.100), 5-hmC (13 eV, 258.044→142.000), 5-fC (256.039→140.0) and 5-caC (272.000→156.000). C, 5-mC, 5-hmC, 5-fC and 5-caC were quantified by calculating the peak area ratio of the analytes and [D_2]-5-hmC. Calibration curves were drawn by measuring the amount of authentic standards spiked with [D_2]-5-hmC. The numbers of C, 5-mC and 5-hmC were calculated by dividing by the moles of total nucleosides.

Analysis of *TET1-3*, *TDG* and *IDH1-2* transcript levels

Details are provided in the supplementary materials (Table S1).

Sequencing analysis

Details are provided in the supplementary materials.

Plasmid construction

Details are provided in the supplementary materials.

Cell culture and transfection

Details are provided in the supplementary materials.

Western blot analysis

Details are provided in the supplementary materials.

DNA dot blot analysis

Details are provided in the supplementary materials.

Statistical analysis

Details are provided in the supplementary materials.

Results

Global 5-mC and 5-hmC levels in GCs

We used the LC-MS/MS method for the quantification of 5-mC, 5-hmC, 5-fC and 5-caC. [D_2]-5-hmC was used as an internal standard. Calibration curves were drawn by measuring the amount of authentic standards spiked with [D_2]-5-hmC (Figure S2). Detection limits for the column were as follows: 5-mC, 0.059 fmol; 5-hmC, 0.057 fmol; 5-fC, 0.103 fmol; and 5-caC, 0.133 fmol. 5-fC and 5-caC were

excluded from subsequent analyses because we could not detect any signal peaks above the detection limits. The resulting calibration curve was used to determine the global levels of C, 5-mC and 5-hmC in 28 pairs of GC tissues. The 5-mC and 5-hmC values were quantified with reference to the quantity of C. As shown in Table S2, 5-mC values ranged from 292.00 modifications per 10^4 C base (292.00/10^4 C) to 430.62/10^4 C, while the 5-hmC values ranged from 1.63/10^4 C to 19.54/10^4 C. The median 5-mC value was 377.92/10^4 C in the normal tissues and 366.66/10^4 C in the cancer tissues, while the median 5-hmC value was 9.63/10^4 C in the normal tissues and 3.32/10^4 C in the cancer tissues. In total 5-mC was moderately decreased in the tumor portions compared with the normal portions (Table S2, $P = 0.021$). 5-hmC was strikingly decreased in the tumor portions of the GC cases (Table S2, $P < 0.001$). The reduction of 5-hmC in the tumor portion was correlated with the N classification (Table 1, $P = 0.018$). No correlation was seen between the reduction of 5-mC in the tumor portion and any of the clinicopathological factors that were examined (Table 1).

For comparison, in terms of the reduction of 5-hmC in the tumor portion, we also performed the same analysis using 5 pairs of gastric cancers and adjacent gastric mucosa from the so-called Gan mouse (K-19-Wnt1/C2mE mouse), which has been established as an inflammation-mediated rodent stomach cancer model [15]. The number of samples that were examined was too small for differences in the 5-mC and 5-hmC values between the tumor portion and the non-tumor portion to reach a statically significant level. However, the 5-hmC level seemed to be lower in the tumorous portion (Figure S3).

Quantification of *TET1-3*, *TDG* and *IDH1-2* transcripts in GCs

Expressions of *TET1-3*, *TDG* and *IDH2* were significantly decreased in the tumor portions of the GC cases compared

Table 1 Comparisons of 5-mC and 5-hmC levels in gastric cancer tissues with adjacent normal tissues of GC patients in different clinicopathological factors

Characteristics	Cases	5-mC			5-hmC		
		Mean (T/N)	SE	*P* value	Mean (T/N)	SE	*P* value
Age							
>60	24	0.950	0.021	0.286	0.344	0.031	0.248
≤60	4	1.008	0.013		0.696	0.246	
Gender							
Male	17	0.980	0.252	0.162	0.356	0.038	0.322
Female	11	0.926	0.250		0.454	0.105	
Location							
Lower	8	0.917	0.026	0.473	0.373	0.048	0.127
Middle	4	0.981	0.015		0.444	0.090	
Upper	12	0.958	0.032		0.284	0.037	
Others[a]	4	-	-		-	-	
T classification							
T1	5	0.937	0.032	0.947	0.190	0.027	0.054
T2	4	0.970	0.015		0.409	0.097	
T3	10	0.968	0.044		0.350	0.049	
T4	9	0.955	0.028		0.551	0.111	
N classification							
N0	10	0.994	0.035	0.523	0.298	0.048	0.018
N1	2	0.936	0.006		0.296	0.061	
N2	6	0.922	0.054		0.272	0.032	
N3	10	0.950	0.021		0.585	0.098	
Stage							
I	5	0.964	0.022	0.679	0.185	0.024	0.070
II	7	0.985	0.054		0.366	0.050	
III	16	0.945	0.022		0.473	0.072	
Histological type							
Intestinal	16	0.952	0.027	0.688	0.378	0.039	0.699
Diffuse	12	0.967	0.026		0.416	0.100	

A two-tailed independent t-test was used when the number of compared groups is 2. ANOVA testing was used when the number of compared groups is more than 3. $P < 0.05$ was considered statistically significant. N: normal tissue; T: tumor tissue. Indicated are the mean of T divided by N, and SE

[a] 4 cases in which the tumor covered all of the lower, middle and upper parts of the stomach